




Article

Design for Sustainability by Additive Manufacturing: A Study of PLA-Based Door Handle Redesign

Nikodmose Moges Gebre , Pasquale Gallo *  and Stefano Rossi 

Department of Industrial Engineering, Università di Trento, Via Sommarive 9, 38123 Trento, Italy; nikodmosemoges.gebre@unitn.it (N.M.G.); stefano.rossi@unitn.it (S.R.)

* Correspondence: pasquale.gallo@unitn.it

Abstract: This paper presents the redesign of a door handle as a case study in applying long-life manufacturing (LLM) principles to the furniture sector, utilizing additive manufacturing with polylactic acid (PLA), a biodegradable and sustainable polymer. The primary objective of this study is to explore the potential of PLA-based components to enhance sustainability, repairability, and durability in everyday furniture items. A door handle was chosen as a representative product to demonstrate the feasibility of this approach. The redesign emphasizes the potential for consumers to 3D print and replace parts as needed, thereby reducing waste and extending product life-cycles. To assess the material's performance, PLA door handles were subjected to degradation tests under UV light exposure and thermal cycles, simulating real-world conditions. The redesigned handles demonstrated a mass reduction of over 50% compared to the original target, while retaining more than 95% of their initial tensile strength after 14 days of UV-B exposure and thermal cycling between 5 °C and 50 °C. The color change remained minimal, particularly for the white-painted samples, indicating satisfactory aesthetic stability. This research contributes to the growing field of sustainable design, highlighting how additive manufacturing can transform the furniture industry by promoting a circular economy through repairable, durable, and eco-friendly solutions.

Keywords: additive manufacturing; long-life manufacturing; sustainability; polylactic acid (PLA); repairability; circular economy; design; green manufacturing



Academic Editor: Mario Farnoli

Received: 8 April 2025

Revised: 21 May 2025

Accepted: 21 May 2025

Published: 28 May 2025

Citation: Gebre, N.M.; Gallo, P.; Rossi, S. Design for Sustainability by Additive Manufacturing: A Study of PLA-Based Door Handle Redesign. *Sustainability* **2025**, *17*, 4969. <https://doi.org/10.3390/su17114969>

Copyright: © 2025 by the authors. Licensee MDPI, Basel, Switzerland. This article is an open access article distributed under the terms and conditions of the Creative Commons Attribution (CC BY) license (<https://creativecommons.org/licenses/by/4.0/>).

1. Introduction

As environmental awareness grows globally, there is increasing demand for manufacturing systems that minimize ecological footprints without compromising functionality or user satisfaction. Traditional product development often prioritizes cost and scalability over longevity and repairability, leading to excessive resource consumption and accelerating product obsolescence. The furniture sector, with its heavy reliance on synthetic materials and standardized mass production, exemplifies these issues. Despite the growing urgency of climate and waste-related challenges, sustainable innovation in furniture design remains relatively underdeveloped. This gap underscores the need for research into alternative production methods and materials that align with circular economy principles. It is within this context that long-life manufacturing (LLM) and additive manufacturing (AM) offer promising avenues for innovation, enabling the creation of customizable, repairable, and environmentally responsible products.

LLM seeks to extend product lifespans through enhanced durability, repairability, and recyclability [1]. Additive manufacturing (AM), also known as 3D printing, allows

for precise, on-demand fabrication, which significantly reduces material waste and energy consumption compared to traditional subtractive methods. Moreover, AM facilitates easy repair and customization of individual parts, empowering users to extend the functional life of furniture products rather than replacing them entirely [2,3]. Fused deposition modeling (FDM) is a widely used additive manufacturing technique (AM) for fabricating various polymeric structures, offering versatility and cost-effectiveness in 3D printing applications [4–7]. Among the materials used in AM, polylactic acid (PLA) has gained attention in the last two decades due to its biodegradability, renewability, low environmental footprint, non-toxicity, biocompatibility with the human body, ease of extrusion at low temperatures, negligible shrinkage, and can be easily processed thermally, as schematically shown in Figure 1 [8–12].

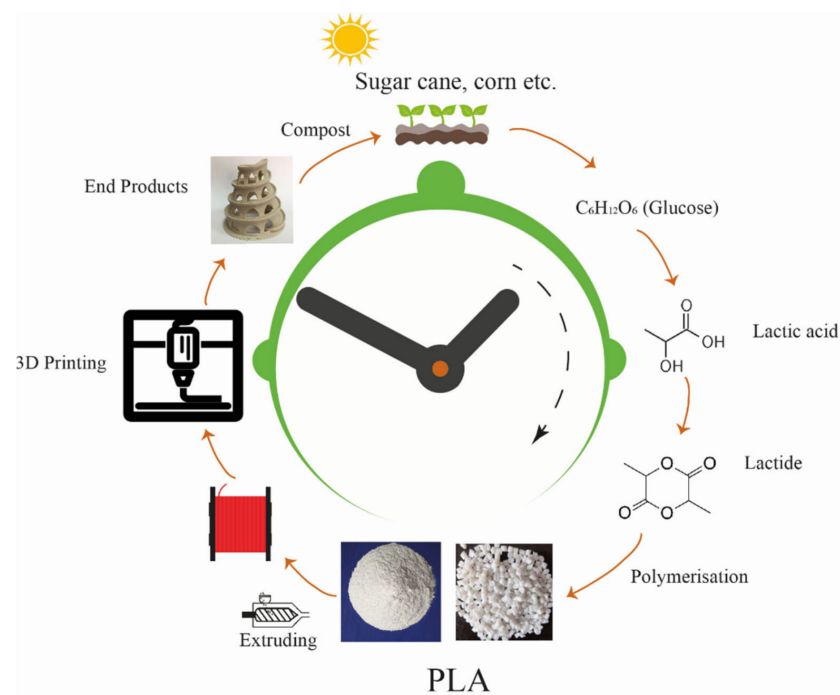


Figure 1. Environmentally friendly polylactic acid (PLA) life-cycle; reproduced from [8] under the CC BY 4.0 license.

The production of PLA polymers is environmentally friendly as they are generally produced by fermentation from the controlled polymerization of lactic acid monomers derived from renewable sources (e.g., corn starch, sugar cane, wheat, and rice), which absorb carbon dioxide during their growth [13–17]. Therefore, PLA offers a viable alternative to conventional polymeric materials in large-scale production industries such as interior design and furniture applications. However, its long-term durability and performance under real-world conditions remain areas of active research [18].

Among various interior design and furniture components, door handles stood out as essential elements that fulfilled multiple functional needs [19,20]. They enhanced aesthetics, ensured comfort, safety, and efficiency, and contributed to ergonomic design. Comprehensive studies on these important topics that affect design decisions can be found in [21–23]. In the modern era, the global door handle market is rapidly growing: valued at USD 7.96 billion in 2024, the market is expected to reach USD 11.59 billion by 2031, as seen in Figure 2 [24–26].

Given this framework, this study aims to advance the concept of LLM within the furniture sector by exploring the potential of AM as an enabler of sustainable product strategies. AM offers unique advantages in this context: the ability to locally reprint dam-

aged components (the repair process is available directly to the user); implement modular design strategies for easier part replacement; enable a high degree of personalization that enhances user attachment and discourages premature disposal, thus promoting LLM; and enabling human-centered design that caters to diverse needs, including those of individuals with varying abilities or life stages, thus again promoting LLM through adaptive personalization. Such possibilities may open new business models in which manufacturers provide open-access libraries of critical components, such as handles, or brackets, allowing consumers to repair or personalize their furniture directly. These elements align with the goals of the circular economy by reducing unnecessary waste and promoting functional longevity. Furthermore, AM technologies offer compatibility with biopolymers such as PLA, which exhibit favorable processing properties and low environmental impact.

For these reasons, this work presents the redesign of a door handle as a representative case study to illustrate how design for AM must account not only for geometric manufacturability but also for structural integrity, durability, and aesthetic preservation under realistic usage conditions: design, material, and performance are strictly integrated. To assess all these aspects, structural analysis of the component was performed to define functional requirements as the first step. The results of this first step have driven the dimensioning of critical features. Subsequently, degradation tests were conducted under UV-B light exposure and thermal cycling conditions to simulate environmental wear and tear. Mechanical properties and aesthetic stability (i.e., color variation and coating degradation) were then evaluated to ensure that the re-engineered PLA handle would retain core functions and the visual appeal of its traditional counterpart. This study emphasizes and demonstrates how innovative production techniques can shift the furniture industry from a traditional linear “use and discard” model to a circular economy, where products are designed for longevity, reparability, and minimal waste without compromises in terms of functionality and aesthetic appeal. This paper, by selecting a door handle, also demonstrates how the concepts briefly discussed can be operationalized and evaluated.

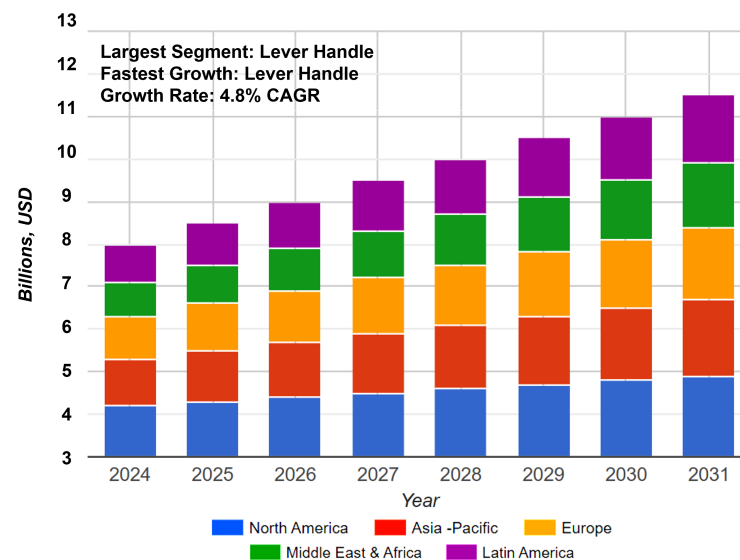


Figure 2. Global door handle market size, trends, share and growth; re-adapted from [25] with permission. Note: CAGR—compound annual growth rate.

2. Materials and Methods

The methodology of the research integrated experimental, analytical, and computational techniques to evaluate and optimize PLA-based components for furniture applications. Standardized mechanical testing [27,28] was conducted to determine tensile proper-

ties, while accelerated degradation protocols—including UV-B radiation exposure [29] and thermal cycling [30] were employed to simulate environmental aging. Surface degradation was quantitatively assessed through colorimetric analysis using a spectrophotometer [31]. Specimens were fabricated using FDM-based additive manufacturing, and design optimization was performed with computer-aided design tools, including Autodesk Inventor Professional 2025 and nTop 5.17.2, for lattice structure integration. Together, these methods provided a comprehensive, multidisciplinary framework for assessing the durability, performance, and sustainability of redesigned PLA door handles. All activities were conducted at the University of Trento.

2.1. Materials

The material of choice for the current work is polylactic acid, better known as PLA. PLA exhibits a glass transition temperature ranging from 55 °C to 65 °C, a melting temperature between 150 °C and 155 °C, and a thermal degradation temperature ranging from 300 °C to 370 °C. The FDM fabrication process was carried out with a Bambu Lab X1-Carbon printer (Shenzhen and Shanghai in China and Austin, Texas in the U.S.), equipped with a 0.4 mm nozzle, operated with a constant layer height of 0.2 mm and a filament diameter of 1.75 mm. The samples were printed with a linear fill pattern ($\pm 45^\circ$) at 100%, as recommended in [14], the bed temperature was set to 55 °C, and the printing temperature was set to 220 °C. The temperature in the printer room was maintained at 37 °C. A commercial PLA filament supplied with the Bambu Lab was used and the as-supplied properties are detailed in Table 1.

Table 1. PLA door handle general material properties [18].

Material	E, GPa	ν	Yield, MPa	UTS, MPa	Density, g/cm ³	Elongation at Break, %
PLA	3.5	0.36	70	73	1.25	7

In addition to the final door handle prototype, two sample geometries were produced, small plates (5 mm × 70 mm × 50 mm) for color characterization [32], and dogbone samples for tensile testing [27,28], as shown in Figure 3 (left) and Figure 3 (right), respectively. The dogbone samples were 3D-printed with a fully solid internal structure, eliminating any internal gaps or filling patterns. This approach provides a uniform distribution of material, maximizes structural integrity, and ensures that mechanical properties such as tensile strength and stiffness can be accurately assessed without interference of internal porosity [33–38]. Since the mechanical performance of PLA can be influenced by moisture, the printer includes a controlled-temperature, filament-drying chamber to maintain material stability. The printing orientation of dogbone samples significantly influences the mechanical property testing. A horizontal layout was chosen as it exhibits greater strength due to improved layer adhesion [14].

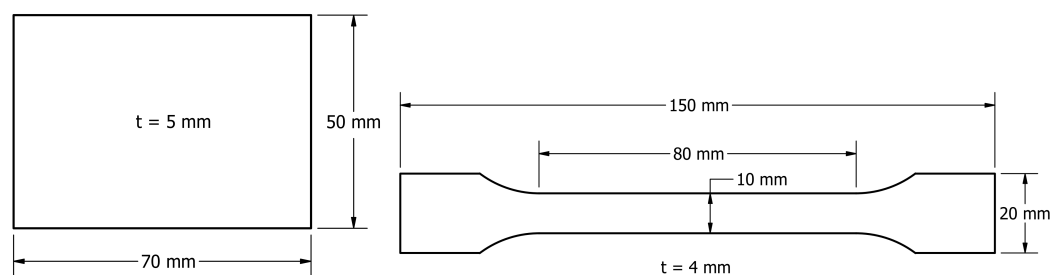


Figure 3. Specimen used in the degradation tests and mechanical characterization; plate sample (left) and dogbone sample (right); t stands for thickness.

The coating was applied for two main purposes: to enhance aesthetics by customizing the product and to assess whether a protective coating is necessary to extend the lifespan of the PLA material. The coating consisted of two layers and was prepared as follows: White paint (waterborne, Franchi and Kim, Castenedolo (BS), Italy) was mixed with a hardener (Franchi and Kim, Castenedolo (BS), Italy) in an 80 % to 20 % ratio. Green paint (acrylic, Arexons, Milan, Italy) was used as a pre-prepared mixture. The thickness of the applied coating was $27.5 \pm 0.5 \mu\text{m}$ for the white paint and $28.5 \pm 3.5 \mu\text{m}$ for the green paint.

2.2. Degradation Tests and Mechanical Characterization

Degradation tests were conducted to evaluate the durability and long-term performance of the PLA door handles, namely UV-B radiation exposure and thermal cycling using a UV173 Box Co.Fo.Me.Gra (Co.Fo.Me.Gra, Milan, Italy) following ASTM 4329-21 standards and using the ACS Thermal Shock Chamber machine (Angelantoni Test Technologies, Massa Martana (PG), Italy), respectively. Plate and dogbone samples were exposed (on both faces) to **UV-B radiation testing** for a duration of 14 days (336 h) to simulate prolonged environmental exposure and assess its effects on the properties of PLA material. UV-B radiation, which falls within the wavelength of 313 nm, is known to accelerate the aging process of polymers by inducing photodegradation, surface oxidation, and changes in mechanical properties [39]. During the exposure period, the samples were placed in a controlled UV chamber with a consistent light intensity (irradiance = 0.6 W/m^2) and temperature of $50 \text{ }^\circ\text{C}$. This controlled setup allowed for a systematic evaluation of how UVB exposure impacts the structural integrity, surface characteristics, and mechanical performance of both coated and uncoated PLA specimens. After the 14-day exposure period, dogbone samples underwent tensile testing and plate samples underwent visual inspection and a color variation test to analyze the extent of degradation and compare the effects of different coatings on the mitigation of UV-B induced damage, according to standards [29,32].

For the **thermal cycling experiment**, plate and dogbone samples were placed in a thermal cycling chamber for 14 days. Both coated and uncoated samples were tested. The thermal machine subjected the samples to repeated heating at $50 \text{ }^\circ\text{C}$ with 90% humidity and cooling at $5 \text{ }^\circ\text{C}$ with 25% humidity, mimicking environmental conditions such as daytime heat and nighttime cooling or seasonal variations, as seen in Figure 4 [30,40]. By exposing both coated and uncoated PLA samples to this thermal treatment, this study aimed to evaluate the impact of different coatings. After the 14-day period, the samples were analyzed by tensile testing, visual inspection, and measurement of color variation to determine any changes in their mechanical performance and surface characteristics.

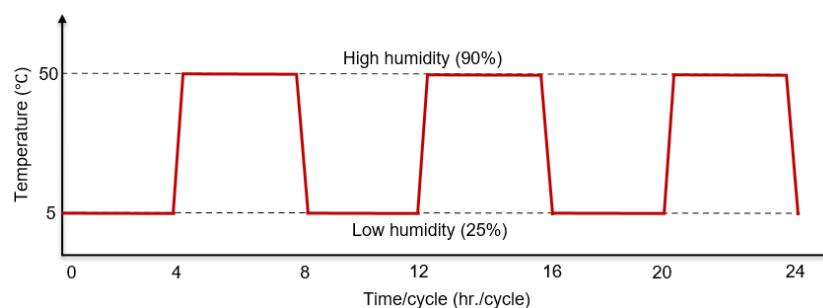


Figure 4. Illustration of a thermal cycle applied to the PLA sample, featuring alternating low- and high-humidity conditions at $5 \text{ }^\circ\text{C}$ and $50 \text{ }^\circ\text{C}$, respectively.

The **color perception measurements** were conducted using the Konica Minolta CM-2600d spectrophotometer (Konica Minolta Sensing Americas, Ramsey, NJ, USA). Data acquisition was performed with a D65 illuminant with a 10° observer angle and a 3 mm

aperture diameter. The measurements align with the CIE Lab* color space system and comply with the ASTM E805 standard. This method utilizes three key coordinates, L^* , a^* , and b^* , which define the color space and provide detailed information on color perception, including hue, lightness, and saturation. Specifically, L^* represents lightness, while a^* and b^* denote chromaticity. Changes along the L^* axis indicate transitions from darker ($-L^*$) to brighter ($+L^*$) shades. Similarly, the a^* and b^* axes represent color directions, where $+a^*$ shifts toward red, $-a^*$ toward green, $+b^*$ toward yellow, and $-b^*$ toward blue. Furthermore, the total color variation (ΔE_{ab}^*) can be calculated using Equation (1) [31,41,42]:

$$\Delta E_{ab}^* = \sqrt{(\Delta L^*)^2 + (\Delta a^*)^2 + (\Delta b^*)^2} \quad (1)$$

To acquire the color coordinates, the instrument's SCE (Specular Component Excluded) measurement mode was selected. This choice ensures that, during accelerated testing, any surface modifications of the coating, such as changes in roughness or texture, can influence the color coordinates, thereby capturing the "true" appearance of the coated plates.

Mechanical testing was carried out on an INSTRON 5969 tensile testing machine (INSTRON, Norwood, MA, USA). Dogbone samples were prepared according to ISO 527-1/2 standards for uniaxial tensile testing [27,28]. The tests were carried out at a speed of 5 mm/min with a 10 kN load cell. The yield stress, Young's modulus, and failure elongation were determined, allowing for a comparison of the effects of UV-B exposure and thermal cycling on PLA material versus net PLA material. An extensometer was used during mechanical testing.

Young's modulus (E_t) was determined from the two stress values (σ_1 and σ_2) corresponding to strain values of 0.0005 and 0.0025 as specified in the ISO 527-1/2 standard [27,28] and shown in Equation (2). The yield stress and elongation at failure were derived from the stress–strain curve. Yield stress represents the first stress at which an increase in strain occurs without an increase in stress, while failure elongation reflects its ductility, which is crucial for evaluating the effects of UV-B exposure and thermal cycling on PLA specimens. To analyze the data results of the tensile tests, the arithmetic mean (\bar{X}) and standard deviation (s) were calculated, as shown in Equations (3) and (4), respectively. The sample standard deviation (s) measures the variability of the data from the mean, indicating a consistent behavior of the material, where x_i is the i -th data point in the dataset and N is the total number of data points.

$$E_t = \frac{\sigma_2 - \sigma_1}{\varepsilon_2 - \varepsilon_1} \quad (2)$$

$$\bar{X} = \frac{x_1 + x_2 + x_3 + \dots + x_N}{N} = \frac{\sum_{i=1}^N x_i}{N} \quad (3)$$

$$s = \sqrt{\frac{\sum_{i=1}^N (x_i - \bar{X})^2}{N - 1}} \quad (4)$$

2.3. Redesign Principles

The methodology for redesigning a sustainable PLA-based handle using additive manufacturing follows several key steps, as shown in Figure 5. First, the mechanical properties and degradation tests of the handle material were performed on the dogbone and plate samples, considering different coatings (see Section 2.2). Then, the mechanical properties of both degraded and non-degraded (i.e., as printed) PLA samples were compared following the ISO 527-1/2 standard. Second, an analysis of existing door handle designs is performed, considering existing designs (size, shape, ergonomics and color), market trends (trends, segmentation, key industrial players), materials (AISI, plastic, glass and wood), manu-

facturing process (shaping, casting and AM), and future design possibilities. Third, the redesign process optimizes the handle's geometry, focusing on its diameter and length, by utilizing solid cylindrical and rectangular cross-sections for both pull and lever types. The objectives are to achieve a mass reduction of 50% and ensure a maximum deflection of less than 20 mm while maintaining optimal cross-sectional dimensions and length restrictions. Finally, a lattice structure is integrated using nTop 5.17.2 (nTop, New York, NY, USA) and AUTODESK Inventor Professional 2025 (Autodesk, San Francisco, CA, USA). The final design application focuses on three types of handles: lever door handles, pull door handles, and drawer handles, ensuring an optimized balance of durability, sustainability, and user comfort. Lever-type door handles feature a ribbed external surface with a body-centered cubic (BCC) lattice infill, whereas pull-type handles are designed in two variations: one with a ribbed external surface and a BCC lattice infill, and the other incorporating a full gyroid lattice structure. Then, water- and oil-based paints are applied.

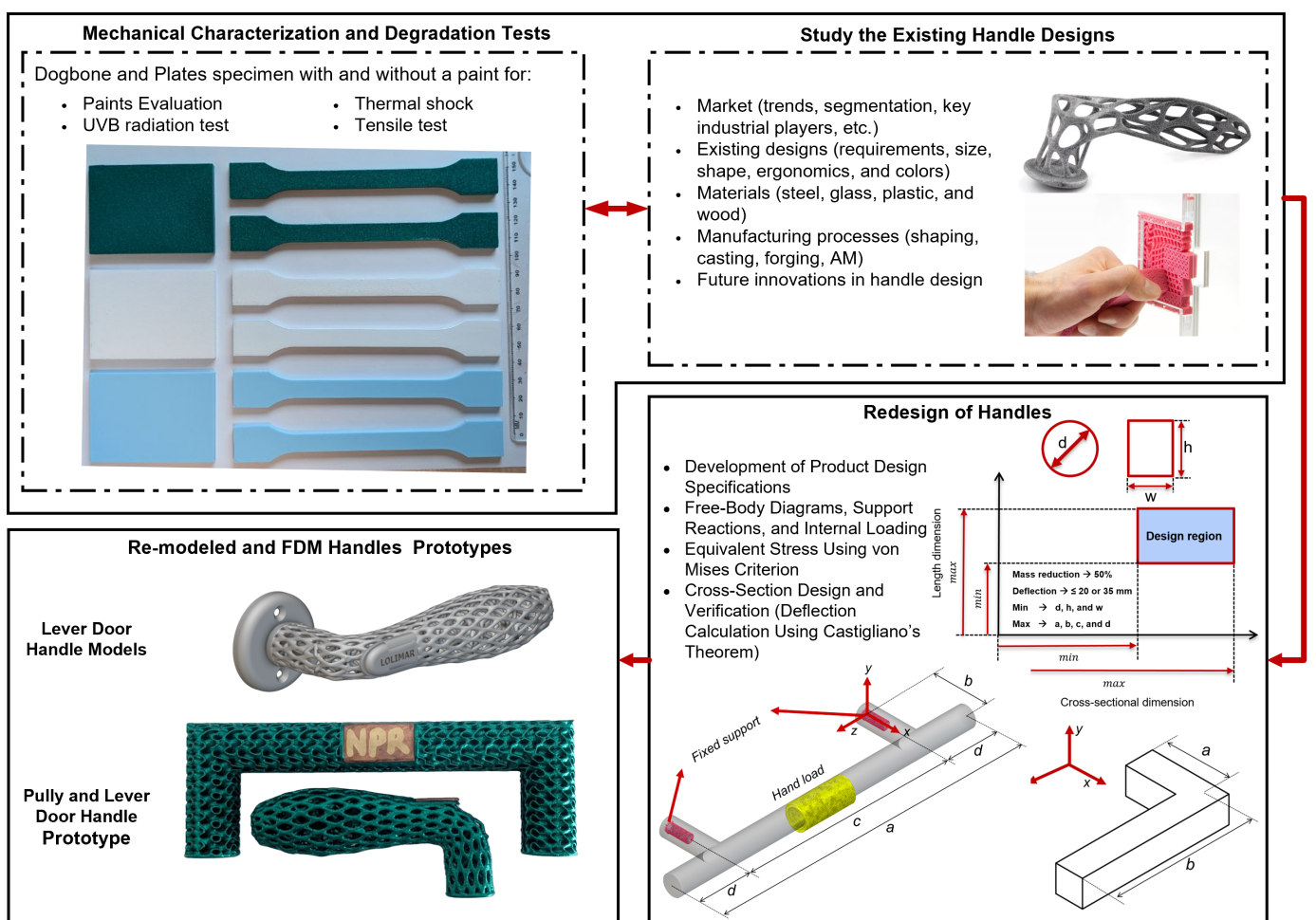


Figure 5. Integrated design methodology for door handle development: from market research and design analysis to material characterization, redesign, and prototyping. Only handle pictures in the upper right sub-figure are taken from [43,44]; all other sub-figures are original. The lower-left sub-figure shows preliminary photos of prototypes developed in this study (a comprehensive picture of the final re-design is provided at the end of the paper).

3. Results and Discussion

Designing and verifying lever and pull door handles requires a blend of ergonomic, aesthetic, and mechanical considerations to ensure functionality and user comfort. These handles are essential in residential, commercial, and industrial environments, where they

must withstand daily use and resist environmental wear (UV radiation and thermal cycle). Consequently, effective lever and pull door handle design involves engineering solutions that prioritize strength, durability, and compliance with safety and accessibility standards.

3.1. Coatings Evaluation

Table 2 and Figure 6 present the colorimetric parameters L^* , a^* , and b^* , along with their respective differences (ΔL^* , Δa^* , Δb^*) and the total color difference ΔE_{ab}^* for uncoated, green-, and white-coated samples under three conditions: unexposed reference (Ref), UV-B exposure (UVB), and thermal aging (TM). A ΔE_{ab}^* value greater than 1 is typically perceptible to the naked eye. These parameters represent lightness, the red–green axis, and the yellow–blue axis, respectively, while ΔL^* , Δa^* , and Δb^* indicate color changes relative to the reference values. For uncoated samples, the lightness (L^*) remains stable after UV-B exposure and thermal cycling (81 to 82). The a^* values shift slightly towards a stronger green tone under UV-B (−18), while thermal cycling retains the initial value (−16). The b^* parameter decreases noticeably after UV-B exposure (−13 to −6), reflecting a reduced bluish tone, with thermal cycling causing only a minor change (−13 to −11). These observations align with the total color difference (ΔE_{ab}^*), which shows a significant change (7.3) after UV-B exposure but a much smaller variation (2.2) due to thermal aging.

Table 2. Effects of UV-B radiation and thermal cycling (TM) on the color parameters (L^* , a^* , b^*) of uncoated, green, and white samples. Note: reference color (Ref); UV-B radiation (UVB); thermal cycling (TM).

Parameters	Uncoated			Green			White		
	Ref	UVB	TM	Ref	UVB	TM	Ref	UVB	TM
L^*	81	82	82	40	40	40	94	94	95
a^*	−16	−18	−16	−48	−39	−48	−2	−1	−1
b^*	−13	−6	−11	12	9	11	2	3	3
ΔL^*	-	−1	−1	-	0	0	-	0	−1
Δa^*	-	2	0	-	−9	0	-	−1	−1
Δb^*	-	−7	2	-	3	1	-	−1	−1
ΔE_{ab}^*	-	7.3	2.2	-	9.5	1	-	1.4	1.7

For the green samples, the lightness (L^*) remains unchanged at 40 under all conditions, indicating stability. However, the value of a^* drops from −48 to −39 after UV-B exposure, indicating reduced greenness, while thermal aging preserves the original color. This is consistent with the values of ΔE_{ab}^* , which show a significant change after exposure to UV-B (9.5) but only a minor variation due to thermal aging (1.0). Lastly, for the white samples, L^* remains stable at 94–95, indicating unchanged brightness. Minor shifts in a^* and b^* suggest slight variations in color balance; however, overall, neither UV-B exposure nor thermal aging significantly affect white color. This is further supported by the low values ΔE_{ab}^* (1.4 for UV-B and 1.7 for TM), confirming minimal perceptible changes in the appearance of the samples. Based on the results, the white waterborne coating provides adequate protection against environmental factors such as UV-B radiation and thermal cycling. Its performance indicates good stability in terms of surface appearance. Therefore, this coating is a promising candidate for outdoor applications that require durability and weather resistance.

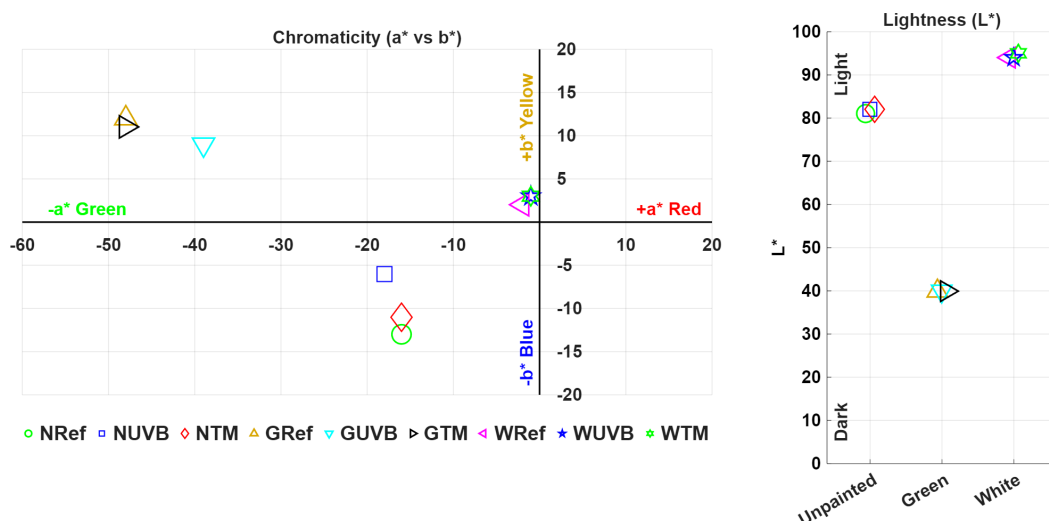


Figure 6. Chromaticity (left) and lightness (right) comparison for untreated (N), coated (green (G) and white (W)), UV exposure (UVB), and thermal cycle (TM) results.

3.2. Mechanical Properties

Table 3 and Figure 7 present the elastic modulus, yield stress, tensile strength at break, and elongation at break for PLA samples subjected to various environmental conditions, including untreated/uncoated (NTT), UV-B exposed (NUVB, GUVB, WUVB) and thermally aged samples (NTM, GTM, WTM). The results highlight distinct mechanical performance trends, with clear degradation in key properties after prolonged UV-B exposure. A pronounced decline is observed after 336 h of UV-B radiation at 310 nm, indicating reducing material degradation and compromised structural integrity.

Table 3. Elastic modulus, yield stress, tensile strength at break, and elongation at break of FDM-printed Dogbone PLA samples. **Note:** NTT denotes untreated and uncoated samples, while UV-B radiation-UVB and thermal cycling-TM samples are categorized as uncoated (N), green (G), and white (W).

Elastic Modulus, GPa							
Sample	NTT	NUVB	GUVB	WUVB	NTM	GTM	WTM
1	2.28	1.41	1.26	1.36	2.10	2.16	2.54
2	2.43	1.34	1.33	1.42	2.35	2.22	2.67
3	2.30	1.33	1.29	1.39	2.05	2.26	2.19
4	2.34	-	-	-	-	-	-
5	2.23	-	-	-	-	-	-
Mean	2.32	1.36	1.29	1.39	2.17	2.21	2.47
S.D.	0.07	0.04	0.03	0.03	0.16	0.05	0.25
Tensile Strength at Yield or Yield Stress, MPa							
Sample	NTT	NUVB	GUVB	WUVB	NTM	GTM	WTM
1	24.7	23.9	23.8	25.2	23.0	23.3	24.6
2	24.6	23.1	23.7	25.4	24.0	22.8	24.8
3	24.4	23.1	23.9	25.2	23.3	22.9	24.1
4	24.4	-	-	-	-	-	-
5	23.8	-	-	-	-	-	-
Mean	24.4	23.4	23.8	25.3	23.4	23.0	24.5
S.D.	0.3	0.5	0.1	0.1	0.5	0.3	0.4

Table 3. Cont.

Tensile Strength at Break, MPa							
Sample	NTT	NUVB	GUVB	WUVB	NTM	GTM	WTM
1	16.7	14.9	19.5	21.6	16.7	16.0	17.2
2	16.1	15.1	19.4	20.6	17.5	15.3	18.4
3	16.2	15.0	18.8	16.4	18.3	15.0	18.0
4	14.4	-	-	-	-	-	-
5	13.5	-	-	-	-	-	-
Mean	15.4	15.0	19.2	19.5	17.5	15.4	17.9
S.D.	1.4	0.1	0.4	2.8	0.8	0.5	0.6
Elongation at Break, %							
Sample	NTT	NUVB	GUVB	WUVB	NTM	GTM	WTM
1	35.2	7.7	11.4	3.9	16.7	20.2	7.2
2	44.1	8.2	11.2	4.8	13.2	12.7	8.7
3	55.6	7.6	11.9	4.3	15.6	15.2	5.8
4	35.4	-	-	-	-	-	-
5	41.4	-	-	-	-	-	-
Mean	42.3	7.8	11.5	4.3	15.2	16.0	7.2
S.D.	8.4	0.3	0.4	0.5	1.8	3.8	1.5

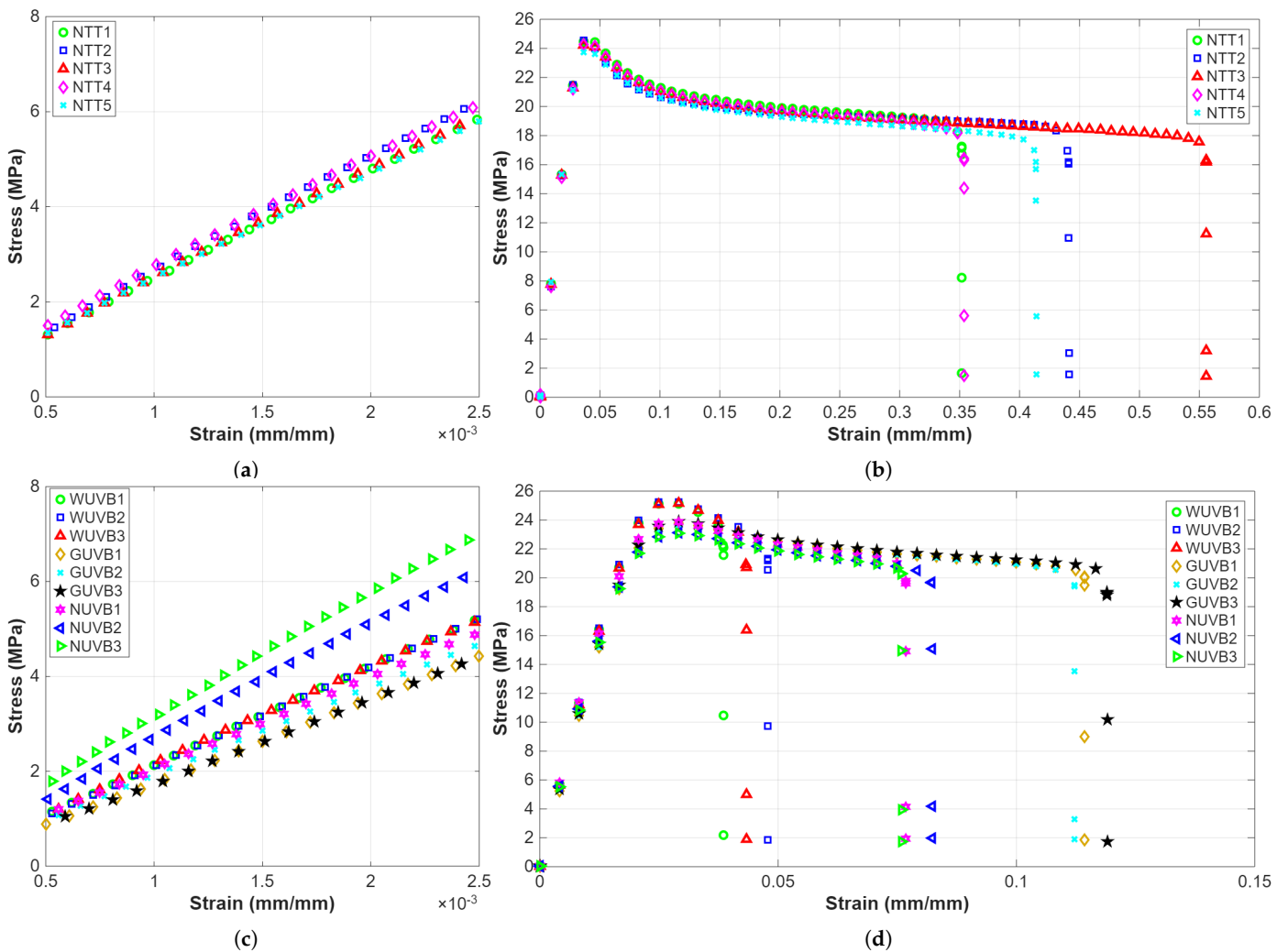


Figure 7. Cont.

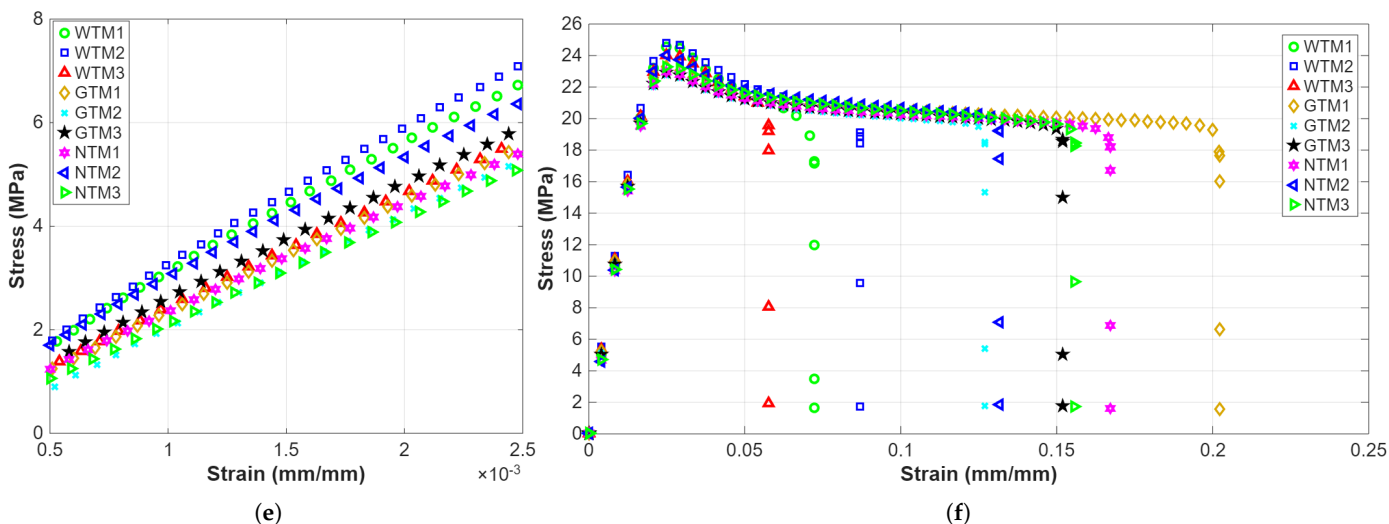


Figure 7. Stress vs. strain diagram illustrating the determination of elastic modulus, yield stress, tensile strength at break, and elongation at break for FDM-printed PLA samples: (a,b) normal samples, (c,d) UV-B exposed samples, and (e,f) thermal cycle exposed samples. Note: NTT denotes untreated and uncoated samples, while UV-B radiation and thermal cycling–TM samples are categorized as uncoated (N), green (G), and white (W).

The virgin uncoated PLA sample (NTT) exhibited the highest elastic modulus compared to older PLA uncoated (NTM) and coated samples exposed to UV-B radiation and thermal cycling as seen in Table 3 and Figure 7. Thermal aging had minimal impact, and UV-B exposure caused a noticeable reduction in elastic modulus, with decreases of 44.4% and 40.1% in the green- and white-painted specimens, respectively. This small decline is attributed to UV-induced photo-oxidation, which weakens the structural integrity of the polymer by breaking molecular chains and leading to micro-crack formation. In contrast, the yield stress values remained relatively stable under different conditions. WUVB showed the highest yield stress (25.3 MPa) with low variability, while NTT samples maintained a consistent strength at 24.4 MPa. Although NUVB exhibited slightly lower yield stress (23.4 MPa) with moderate variability, overall trends indicate that UV-B exposure and thermal aging caused only minor changes in tensile strength. It should be noted that the underlying mechanisms of the declining mechanical properties are not the focus of the current work. Moreover, these mechanisms have been studied extensively for PLA; details are available in [45–47].

WUVB samples had the highest average tensile strength at break (19.5 MPa), followed closely by GUVB (19.2 MPa), while NUVB showed a lower mean of 15.0 MPa. Most samples exhibited low variability, though WUVB had a higher standard deviation (2.8 MPa). The elongation at break showed the largest variation, with the NTT samples demonstrating the highest average value (42.3%), indicating superior ductility. In contrast, WUVB samples exhibited the lowest elongation (4.3%), signifying increased brittleness. NTM and GTM samples showed moderate elongation values (15.2% and 16.0%), reflecting a balance between flexibility and mechanical strength.

3.3. Redesign of Door Handle

Designing and verifying lever and pull door handles requires a careful balance of ergonomic, aesthetic, and mechanical factors to ensure optimal functionality and user comfort, while also withstanding the demands of daily use in residential, commercial, and industrial environments. The design and analysis results for the lever and door handle components are summarized in Table 4. The cross-sectional dimensions—diameter (d_{ABmin} ,

d_{BCmin}), width (w_{ABmin} , w_{BCmin}) and height (h_{ABmin} , h_{BCmin})—as well as the general geometric profiles (a_{max} , b_{max} , c_{max} and d_{max}) are illustrated in the bottom-right corner of Figure 5. These results emphasize the need for engineering design strategies that optimize structural integrity and durability while ensuring compliance with safety and accessibility standards, particularly in terms of rotational deflection and overall mass of the handle designs.

Table 4. Design analysis results for Lever and Pull door handle components (refer to Figure 5 for symbol definitions.)

Design Parameters	Lever	Pull
a_{max} , mm	50	375
b_{max} , mm	200	60
c_{max} , mm	-	250
d_{max} , mm	-	62.5
d_{ABmin} , mm	20	25
d_{BCmin} , mm	20	25
w_{ABmin} , mm	15	17.5
h_{ABmin} , mm	30	35
w_{BCmin} , mm	10	17.5
h_{BCmin} , mm	20	35
Rotation under the load, $\delta_{circular}$, mm	12.6	33.1
Rotation under the load, $\delta_{rectangular}$, mm	10.7	25.2
Mass ($m_{circular}$), g	78	304
Mass ($m_{rectangular}$), g	98	379

To evaluate the performance of the newly designed door handle, the results were compared with those of AISI 304, which is sometimes used for door handles, while maintaining the same cross-sectional area and geometric profile. The mass of AISI 304 lever door handles was 628.3 g for the circular cross-section and 900 g for the rectangular cross-section. For pull door handles, the mass was 1943.9 g and 2425.5 g for the circular and rectangular cross-sections, respectively. In comparison, the mass of PLA lever door handles was significantly lower, weighing 78 g for the circular cross-section and 98 g for the rectangular cross-section. For pull door handles, the mass was 304 g and 379 g for the circular and rectangular cross-sections, respectively. This resulted in a mass reduction of more than 50% compared to the target mass. The rotational deflection of the PLA lever and pull door handles was 12.6 mm and 33.1 mm for the circular cross-section and 10.7 mm and 25.2 mm for the rectangular cross-section, respectively. All values are below the required rotational deflection limits of 20 mm for lever handles and 35 mm for pull handles. When the rotational deflection of PLA is compared with that of AISI 304, it is significantly higher. This is because AISI 304, being a stronger and more rigid material, exhibits less deflection under the same conditions, despite its higher mass.

Based on these insights (as shown in Table 4), the remolding process was conducted for three types of handles (see Figure 8)—lever door handles, pull door handles, and drawer handles—ensuring an optimized balance of durability, sustainability, and user comfort. Lever-type door handles feature a ribbed external surface with a body-centered cubic (BCC) lattice infill, while the pull-type handles are designed in two variations: one with a ribbed external surface and a BCC lattice infill, and the other incorporating a full gyroid lattice structure. Finally, handle types are coated with waterborne and acrylic-based paints for enhanced durability and aesthetic appeal.

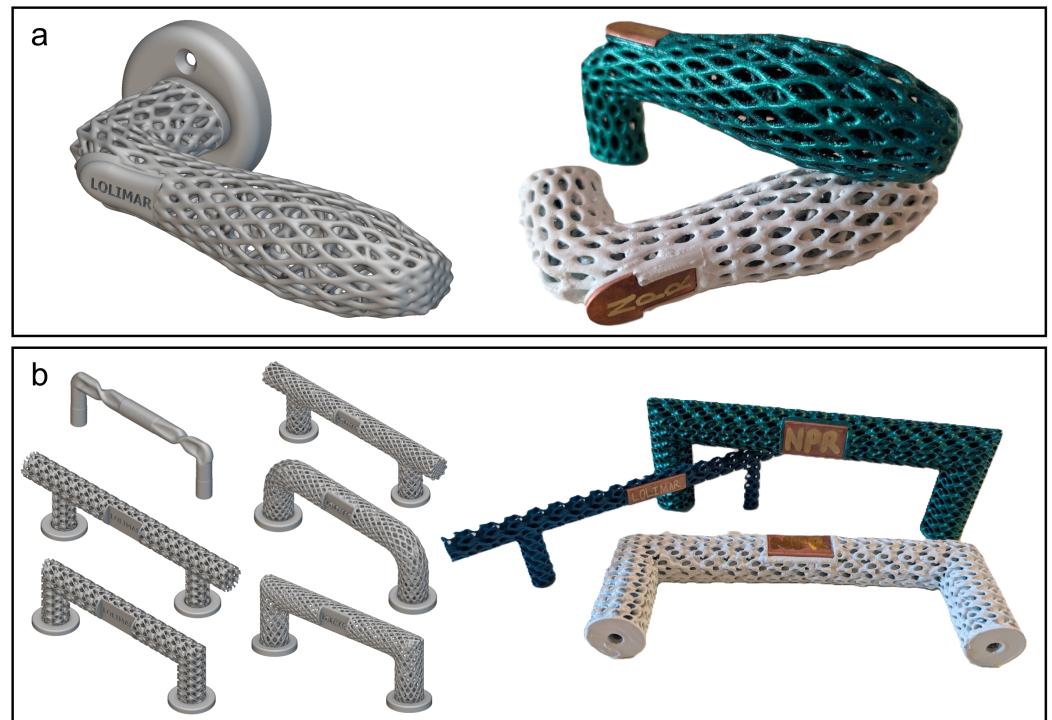


Figure 8. Re-modeled handles fabricated using FDM technology: (a) lever handle showing both CAD design and printed prototype; (b) pull door handles and drawer handles. Both models incorporating lattice structures to enhance aesthetics and reduce material usage.

3.4. Long-Life Manufacturing: Final Considerations

The findings of this study align closely with the principles of long-life manufacturing (LLM), which emphasize the extension of product lifespans through thoughtful, sustainable design. By leveraging biodegradable and recyclable materials like PLA, alongside modular and lattice-based design strategies enabled by additive manufacturing (AM), this research demonstrates how durability and adaptability can be achieved with minimal material consumption.

Durability was enhanced without an excessive use of materials, and the lightweight design, compared to conventional metal handles, resulted in lower resource use and reduced energy demand during production. Furthermore, the modular architecture allows individual components to be repaired or replaced, promoting ease of maintenance and minimizing full-product disposal. This is especially significant in the context of a circular economy, where maintenance and reuse are prioritized over discarding.

When it comes to the design and the process, AM enables several factors to contribute directly to LLM, such as the reparability. For example, the handle could be made of several separate features, so that the most critical and those prone to breaking could be simply printed and replaced with easy assembly; thanks to AM, the concept of repair is not restricted to the company but available to the user who can print what is needed, when it is needed. Another key factor is the personalization enabled by AM. Architects and designers underline that the personal attachment to an object and emotional involvement are directly correlated with the level of personalization: the more unique the handle, the more the user is attached to it. This means that users will rather seek repair rather than replacement.

LLM is also promoted by material selection. A key advantage of using PLA is its potential for recyclability and reusability. In the event of damage, broken handle parts can be reprinted locally, minimizing downtime and material waste. Additionally, PLA components can be recycled. The filament can be melted down and reused for future prints, as outlined in the literature [48,49]. Research indicates that PLA can typically be recycled

and reused up to two to five times before significant degradation in mechanical properties occurs, depending on the quality of the recycled material and processing method [11,12].

These characteristics establish a strong connection between LLM and reparability. Additive manufacturing facilitates localized, on-demand production, empowering users to extend product life through self-service and personalization. This not only supports sustainability but also fosters greater emotional attachment, which has been shown to increase product longevity. Together, these approaches present a compelling case for integrating LLM into consumer products, encouraging innovation in the furniture sector by offering customizable, long-lasting, and environmentally responsible alternatives to traditional manufacturing.

4. Conclusions

This paper summarizes the steps in the redesign of a door handle using FDM-printed polylactic acid (PLA), a biodegradable and sustainable biopolymer. Experimental tests and redesign considerations were presented. The conclusions are summarized as follows:

- UV-B exposure affected color stability, particularly in uncoated and green PLA samples, highlighting the critical need for UV-resistant coatings to preserve aesthetic quality in outdoor applications, whereas thermal aging exhibited only a minor effect across all samples.
- Prolonged UV-B exposure reduced the elastic modulus and elongation at break due to photo-oxidation and the formation of micro-cracks, indicating that surface protection is vital for mechanical resilience in exterior applications. In contrast, thermal cycling had a lesser impact on mechanical properties, except for a noticeable reduction in elongation at break. Overall, both UV-B and thermal aging led to a clear reduction in ductility, with UV-B exposure also causing an increase in tensile strength but further compromising ductility.
- Through the use of lattice infill optimization and protective coatings, the redesigned lever, pull, and drawer handles achieved an optimal balance of weight reduction, strength, aesthetics, and ergonomics, while additive manufacturing further enabled lightweight, repairable, and customizable designs that foster user engagement, emotional attachment, and extended product life in alignment with LLM principles.

As a future work, life cycle assessment, cost estimation, and reliability of printing process will be addressed.

Author Contributions: Conceptualization, N.M.G., P.G. and S.R.; investigation and formal analyses, N.M.G.; writing—original draft preparation, N.M.G. and P.G.; writing—review and editing, N.M.G., P.G. and S.R.; supervision, P.G.; resources, S.R. All authors have read and agreed to the published version of the manuscript.

Funding: This study was funded by the European Union—Next Generation EU—PNRR, Mission 4 Component 2, Investment 1.3—PE MICS Spoke 5—LOLIMAR Project (PE00000004, CUP D43C22003120001).

Data Availability Statement: The original contributions presented in this study are included in this article. Further inquiries can be directed to the corresponding author.

Acknowledgments: We extend our gratitude to Daniele Rigotti from the Polymer Lab (DII, University of Trento), as well as Luca Benedetti from the Coating and Corrosion Laboratory (DII, University of Trento). We also sincerely thank Francesca Russo (DII, University of Trento) for her support.

Conflicts of Interest: The authors declare no conflicts of interest.

Abbreviations

a^* and b^*	Chromaticity
ΔE_{ab}^*	Total color variation
L^*	Lightness
AM	Additive manufacturing
CAGR	Compound annual growth rate
FDM	Fused deposition modeling
G	Green
LLM	Long-life manufacturing
N	Untreated or uncoated
PLA	Polylactic acid
Ref	Reference color
TM	Thermal cycle
UV-B	Ultraviolet B radiation
W	White

References

- Montalvo, C.; Rietveld, E.; Peck, D. A Longer Lifetime for Products: Benefits for Consumers and Companies. June 2016. Available online: <https://www.researchgate.net/publication/305043294> (accessed on 1 May 2025).
- ASTM F2792-12a; Terminology for Additive Manufacturing Technologies. ASTM: West Conshohocken, PA, USA, 2012. <https://doi.org/10.1520/F2792-12A>.
- Din, I.U.; Kulkarni, S.S.; Khan, K.A. Thermo-Mechanical viscoelastic Characterization and Modeling of 4D Printed Shape Memory Polymers. *Polym. Test.* **2025**, *143*, 108708. <https://doi.org/10.1016/j.polymertesting.2025.108708>.
- Storck, J.L.; Ehrmann, G.; Uthoff, J.; Diestelhorst, E.; Blachowicz, T.; Ehrmann, A. Investigating Inexpensive Polymeric 3D Printed Materials Under Extreme Thermal Conditions. *Mater. Futur.* **2022**, *1*, 015001. <https://doi.org/10.1088/2752-5724/ac4beb>.
- Guessasma, S.; Belhabib, S.; Nouri, H. Thermal Cycling, Microstructure and Tensile Performance of PLA-PHA Polymer Printed Using Fused Deposition Modelling Technique. *Rapid Prototyp. J.* **2020**, *26*, 122–133. <https://doi.org/10.1108/RPJ-06-2019-0151>.
- Djurović, S.; Lazarević, D.; Ćirković, B.; Mišić, M.; Ivković, M.; Stojčević, B.; Petković, M.; Ašonja, A. Modeling and Prediction of Surface Roughness in Hybrid Manufacturing–Milling After FDM Using Artificial Neural Networks. *Appl. Sci.* **2024**, *14*, 5980. <https://doi.org/10.3390/app14145980>.
- Palić, N.; Slavković, V.; Živana Jovanović.; Živić, F.; Grujović, N. Mechanical Behaviour of Small Load Bearing Structures Fabricated by 3D Printing. *Appl. Eng. Lett.* **2019**, *4*, 88–92. <https://doi.org/10.18485/aeletters.2019.4.3.2>.
- Tümer, E.H.; Erbil, H.Y. Extrusion-Based 3d Printing Applications of PLA Composites: A Review. *Coatings* **2021**, *11*, 390. <https://doi.org/10.3390/coatings11040390>.
- Podzorova, M.V.; Tertyshnaya, Y.V.; Pantyukhov, P.V.; Popov, A.A.; Nikolaeva, S.G. Influence of Ultraviolet on Polylactide Degradation. In Proceedings of the International Conference on Advanced Materials with Hierarchical Structure for New Technologies and Reliable Structures, Tomsk, Russia, 9–13 October 2017; American Institute of Physics Inc.: Melville, NY, USA, 2017; Volume 1909. <https://doi.org/10.1063/1.5013854>.
- Brown, M.H.; Badzinski, T.D.; Pardoe, E.; Ehlebracht, M.; Maurer-Jones, M.A. UV Light Degradation of Polylactic Acid Kickstarts Enzymatic Hydrolysis. *Acs Mater.* **2024**, *4*, 92–98. <https://doi.org/10.1021/acsmaterialsau.3c00065>.
- Lanzotti, A.; Martorelli, M.; Maietta, S.; Gerbino, S.; Penta, F.; Gloria, A. A Comparison Between Mechanical Properties of Specimens 3D Printed with Virgin and Recycled PLA. *Procedia Cirp* **2019**, *79*, 143–146. <https://doi.org/10.1016/j.procir.2019.02.030>.
- Hidalgo-Carvajal, D.; Álvaro Hortal Muñoz.; Garrido-González, J.J.; Carrasco-Gallego, R.; Montero, V.A. Recycled PLA for 3D Printing: A Comparison of Recycled PLA Filaments from Waste of Different Origins after Repeated Cycles of Extrusion. *Polymers* **2023**, *15*, 3651. <https://doi.org/10.3390/polym15173651>.
- Bhagwat, S.V.; Shukla, V.V.; Trivedi, M.G.; Jha, A.; Padole, P. An Engineering Investigation of Bio-Polymers. *Int. J. Mech. Prod. Eng. Res. Dev.* **2019**, *9*, 348–355. Available online: <https://www.researchgate.net/publication/335910272> (accessed on 1 May 2025).
- Corapi, D.; Morettini, G.; Pascoletti, G.; Zitelli, C. Characterization of a Polylactic Acid (PLA) Produced by Fused Deposition Modeling (FDM) Technology. *Procedia Struct. Integr.* **2019**, *24*, 289–295. <https://doi.org/10.1016/j.prostr.2020.02.026>.
- Zhang, C.; Rathi, S.; Goddard, J.; Constantine, K.; Collins, P. The Effect of UV Treatment on the Degradation of Compostable Polylactic Acid. *J. Eng. Investig.* **2013**. <https://doi.org/10.59720/13-023>.

16. McKeown, P.; Jones, M.D. The Chemical Recycling of PLA: A Review. *Sustain. Chem.* **2020**, *1*, 1–22. <https://doi.org/10.3390/suschem1010001>.
17. Beltrán, F.R.; Arrieta, M.P.; Moreno, E.; Gaspar, G.; Muneta, L.M.; Carrasco-Gallego, R.; Yáñez, S.; Hidalgo-Carvajal, D.; de la Orden, M.U.; Urreaga, J.M. Evaluation of the Technical Viability of Distributed Mechanical Recycling of PLA 3D Printing Wastes. *Polymers* **2021**, *13*, 1247. <https://doi.org/10.3390/polym13081247>.
18. Farah, S.; Anderson, D.G.; Langer, R. Physical and Mechanical Properties of PLA, and their Functions in Widespread Applications—A Comprehensive Review. *Adv. Drug Deliv. Rev.* **2016**, *107*, 367–392. <https://doi.org/10.1016/j.addr.2016.06.012>.
19. Bairagi, A.R.; Bisht, D.S. Design of Door Handle. Doctoral Dissertation, National Institute of Technology, Rourkela, India, 2014. Available online: <https://core.ac.uk/download/pdf/53190392.pdf> (accessed on 1 May 2025).
20. Dorsey, O. Improvement In Door Holding Devices. 1878. Available online: <https://patents.google.com/patent/US210764A/en> (accessed on 1 May 2025).
21. Deeb, J.M.; Danz-Reece, M.E.; Attwood, D.A. *Ergonomic Solutions for the Process Industries*; Gulf Professional Publishing, Elsevier: Amsterdam, The Netherlands, 2004.
22. Paschoarelli, L.C.; Santos, R.; Bruno, P. Influence of Door Handles Design in Effort Perception: Accessibility and Usability. *Work* **2012**, *41*, 4825–4829. <https://doi.org/10.3233/WOR-2012-0771-4825>.
23. Brass, C.; Glutz. *GAI-Guide to Standards-10-BSEN1906-22-Final*; Technical Report; Guild of Architectural Ironmongers: London, UK, 2012.
24. Versha, V. Door Handles Market Size, Share, Growth and Industry Analysis. Technical Report, King Research. 2024. Available online: <https://www.kingsresearch.com/door-handles-market-384> (accessed on 1 May 2025).
25. Skyquest. Global Door Handles Market. Technical Report, Skyquest. 2024. Available online: <https://www.skyquestt.com/report/door-handles-market> (accessed on 1 May 2025).
26. Varma, J.; Patankar, N. Door Handles Market: Market Analysis 2017–2030. Technical Report, Grand View Research. 2021. Available online: <https://www.grandviewresearch.com/industry-analysis/door-handles-market> (accessed on 1 May 2025).
27. ISO-527-1; Determination of Tensile Properties. ISO: Geneva, Switzerland, 1993.
28. ISO-527-2; Determination of Tensile Properties. ISO: Geneva, Switzerland, 1993.
29. ASTM D4329-21; Practice for Fluorescent Ultraviolet (UV) Lamp Apparatus Exposure of Plastics. ASTM: West Conshohocken, PA, USA, 2021. <https://doi.org/10.1520/D4329-21>.
30. IEC 60068-2-14; International Standard Norme International Environmental Testing-Part 2-14. IEC: Geneva, Switzerland, 2023. Available online: <https://standards.iteh.ai/catalog/standards/sist/3b4877b9-523b-4b80-b18b-6fc4d202bdc0/iec-> (accessed on 1 May 2025).
31. ASTM E805; Practice for Identification of Instrumental Methods of Color or Color-Difference Measurement of Materials. ASTM: West Conshohocken, PA, USA, 2022. <https://doi.org/10.1520/E0805-22>.
32. ASTM D4674-19; Practice for Accelerated Testing for Color Stability of Plastics Exposed to Indoor Office Environments. ASTM: West Conshohocken, PA, USA, 2019 <https://doi.org/10.1520/D4674-19>.
33. Othman, M.S.; Misran, M.F.R.; aba Helmi Khamisan. Study on Mechanical Properties of PLA Printed using 3D Printer. *J. Adv. Res. Appl. Mech. J.* **2019**, *59*, 10–18. Available online: <https://www.researchgate.net/publication/346713811> (accessed on 1 May 2025).
34. Singh, J.; Goyal, K.K.; Kumar, R. Effect of Filling Percentage and Raster Style on Tensile Behavior of FDM Produced PLA Parts at Different Build Orientation. *Mater. Today Proc.* **2022**, *63*, 433–439. <https://doi.org/10.1016/j.matpr.2022.03.444>.
35. Gunasekaran, K.N.; Aravindh, V.; Kumaran, C.B.; Madhankumar, K.; Kumar, S.P. Investigation of Mechanical Properties of PLA Printed Materials Under Varying Infill Density. *Mater. Today Proc.* **2021**, *45*, 1849–1856. <https://doi.org/10.1016/j.matpr.2020.09.041>.
36. Hanon, M.M.; Dobos, J.; Zsidai, L. The Influence of 3D Printing Process Parameters on the Mechanical Performance of PLA Polymer and its Correlation with Hardness. *Procedia Manuf.* **2020**, *54*, 244–249. <https://doi.org/10.1016/j.promfg.2021.07.038>.
37. Akhil, V.M.; Aravind, S.L.; Kiran, R.; Sivapirakasam, S.P.; Mohan, S. Experimental Investigations on the Effect of Infill Patterns on PLA for Structural Applications. *Mater. Today Proc.* **2022**, *76*, 636–639. <https://doi.org/10.1016/j.matpr.2022.10.292>.
38. Yao, T.; Ye, J.; Deng, Z.; Zhang, K.; Ma, Y.; Ouyang, H. Tensile Failure Strength and Separation Angle of FDM 3D Printing PLA Material: Experimental and Theoretical Analyses. *Compos. Part Eng.* **2020**, *188*, 107894. <https://doi.org/10.1016/j.compositesb.2020.107894>.
39. Sun, J.; Wang, X.; Zheng, H.; Xiang, H.; Jiang, X.; Fan, J. Characterization of the Degradation Products of Biodegradable and Traditional Plastics on UV Irradiation and Mechanical Abrasion. *Sci. Total Environ.* **2024**, *909*, 168618. <https://doi.org/10.1016/j.scitotenv.2023.168618>.
40. ACS. Thermal Shock Chambers. Technical Report, Angelantoni Technology for Life. 2014. Available online: <https://www.acstestchambers.com/en/environmental-test-chambers/air-to-air-thermal-shock-chambers/> (accessed on 1 May 2025).

41. Ramdé, T.; Ecco, L.G.; Rossi, S. Visual Appearance Durability as Function of Natural and Accelerated Ageing of Electrophoretic Styrene-acrylic Coatings: Influence of Yellow Pigment Concentration. *Prog. Org. Coatings* **2017**, *103*, 23–32. <https://doi.org/10.1016/j.porgcoat.2016.11.028>.
42. Ecco, L.G.; Rossi, S.; Fedel, M.; Deflorian, F. Color Variation of Electrophoretic Styrene-acrylic Paints Under Field and Accelerated Ultraviolet Exposure. *Mater. Des.* **2017**, *116*, 554–564. <https://doi.org/10.1016/j.matdes.2016.12.051>.
43. 3DPrint. Door Handle PA12. 2025. Available online: <https://www.martinpierce.com/blog/category/casting+process> (accessed on 1 May 2025).
44. Ion, A.; Frohnhofen, J.; Wall, L.; Kovacs, R.; Alistar, M.; Lindsay, J.; Lopes, P.; Chen, H.T.; Baudisch, P. Metamaterial Mechanisms. In Proceedings of the 29th Annual ACM Symposium on User Interface Software and Technology (UIST '16), ACM, Tokyo, Japan, 16–19 October 2016. <https://dl.acm.org/doi/10.1145/2984511.2984540>.
45. Chopra, S.; Pande, K.; Puranam, P.; Deshmukh, A.D.; Bhone, A.; Kale, R.; Galande, A.; Mehtre, B.; Tagad, J.; Tidake, S. Explication of Mechanism Governing Atmospheric Degradation of 3D-printed Poly(lactic acid) (PLA) with Different in-fill Pattern and Varying In-fill Density. *Rsc Adv.* **2023**, *13*, 7135–7152. <https://doi.org/10.1039/d2ra07061h>.
46. Shi, L.K.; Li, P.C.; Liu, C.R.; Zhu, J.X.; Zhang, T.H.; Xiong, G. An Improved Tensile Strength and Failure Mode Prediction Model of FDM 3D Printing PLA Material: Theoretical and Experimental Investigations. *J. Build. Eng.* **2024**, *90*, 109389. <https://doi.org/10.1016/j.jobe.2024.109389>.
47. Amza, C.G.; Zapciu, A.; Baci, F.; Vasile, M.I.; Nicoara, A.I. Accelerated Aging Effect on Mechanical Properties of Common 3D-Printing Polymers. *Polymers* **2021**, *13*, 4132. <https://doi.org/10.3390/polym13234132>.
48. Moreno, E.; Beltrán, F.R.; Arrieta, M.P.; Gaspar, G.; Muneta, L.M.; Carrasco-Gallego, R.; Yáñez, S.; Hidalgo-Carvajal, D.; de la Orden, M.U.; Urreaga, J.M. Technical Evaluation of Mechanical Recycling of PLA 3D Printing Wastes. *Proceedings* **2021**, *69*, 19. <https://doi.org/10.3390/cgpm2020-07187>.
49. Hasan, M.R.; Davies, I.J.; Pramanik, A.; John, M.; Biswas, W.K. Potential of Recycled PLA in 3D Printing: A Review. *Sustain. Manuf. Serv. Econ.* **2024**, *3*, 100020. <https://doi.org/10.1016/j.smse.2024.100020>.

Disclaimer/Publisher's Note: The statements, opinions and data contained in all publications are solely those of the individual author(s) and contributor(s) and not of MDPI and/or the editor(s). MDPI and/or the editor(s) disclaim responsibility for any injury to people or property resulting from any ideas, methods, instructions or products referred to in the content.